ASTRONOMY & ASTROPHYSICS
SUPPLEMENT SERIES

DECEMBER 1989, PAGE 353

Astron. Astrophys. Suppl. Ser. **81**, 353-365 (1989)

Near infrared spectra of galactic and magellanic Wolf-Rayet stars (*)

J. M. Vreux (1, 2), M. Dennefeld (3), Y. Andrillat (4) and K. Rochowicz (1, 5)

(1) Institut d'Astrophysique, 5, avenue de Cointe, B-4200 Cointe Ougrée, Belgium
(2) Joint Institute for Laboratory Astrophysics, University of Colorado, Boulder, Colorado 80309, U.S.A.
(3) Institut d'Astrophysique, 98 bis, Boulevard Arago, F-75014 Paris, France
(4) Laboratoire d'Astronomie, (C.N.R.S. : U.R.A. 1281, Observatoire du Pic du Midi), Université des Sciences Montpellier II, F-34060 Montpellier, Cedex 1, France
(5) Institut d'Astronomie, Université Nicolas Copernicus, Torun, Poland

Received June 16, accepted September 1, 1989

Summary. — The first part of this paper presents near infrared spectra (λ 6150 - λ 10350 Å) of galactic and mainly Magellanic Wolf Rayet Stars. The spectra are compared to the ones published previously in the "Catalogue of near infrared spectra of southern galactic WR stars" and some peculiarities are pointed out. In the second part, the hydrogen signature in the Paschen series is discussed. For all the galactic and Magellanic objects in which such a signature could be quantified, a value of the H^+/He^{++} ratio has been derived and compared to previous estimations based on the Balmer series.

Key words : stars : Wolf Rayet — spectrophotometry — near infrared.

1. Introduction.

Despite their tremendous influence on the life of a galaxy (see for example Abbott and Conti, 1987, or van der Hucht *et al.*, 1987), the Wolf Rayet (hereafter WR) stars remain rather mysterious (see for example their last wandering in the HR diagram according to Schmutz *et al.*, 1989). Their classification scheme is based on the appearance of a few optical emission lines of ions of helium, carbon, nitrogen and oxygen which tell us more about the dense wind blowing from these objects than on the underlying star itself. Recently, important improvements have been made in the modelling of the helium spectra of the WR stars via calculations taking into account non-LTE radiation transfer in spherically expanding atmospheres (Wessolowski *et al.*, 1988). While such attempts are pursued on the theoretical side, parallel efforts can be made from the observational one. They imply a more quantitative description of the spectra (allowed now by the use of "linear detectors", see for exemple Conti and Massey, 1989) as well as the full use of all the spectral ranges accessible, which reveal information on layers located at different depths in the wind. From a purely observational point of view this should lead to a better definition of the different aspects of the WR phenomena and allow one to tackle problems like the large heterogeneity of line strengths in a given subtype (Conti *et al.*, 1983). This could be compulsory if one wants to improve the use of these objects as tracers of the galactic environments. Such a framework will also constitute a test bench as progress are made in the theoretical modelling.

In this context, our efforts were devoted to the λ 6000 to λ 10350 Å region, i.e. the spectral domain connecting the visible to the region accessible to the photovoltaïc indium antimonide detectors. In addition to line identifications in that spectral range, the aim of our first paper (Vreux *et al.*, 1983 ; hereafter VDA) was to provide a representative spectrum as well as quantitative information on the main emissions for nearly each subtype of galactic WR stars. With the progress going on in the modelling of WR spectra, we have decided to improve this first approach in three directions :

- the observations of Magellanic stars ;
- the illustration in the near infrared region of the heterogeneity which can exist in a given subtype ;

(*) All the observations reported here have been collected at the European Southern Observatory (ESO) at La Silla, Chile.
Send offprint requests to : J. M. Vreux.

– the study of the signature of hydrogen in the Paschen region.

2. Observations.

The observations reported here have been performed with the ESO Reticon system (Dennefeld *et al.*, 1979) attached to the Boller and Chivens spectrograph at the 3.6 m ESO telescope on La Silla (Chile).

Table I lists the stars selected for the present paper ; the first column gives the spectral type from the catalogues referred to below, the second the identification number in Breysacher's thesis (1988) for the LMC and SMC stars, and in van der Hucht *et al's* catalogue (1981) for the galactic ones. The next columns respectively give the HD number, the visual magnitude (as given in the catalogues mentionned above), the date of the observation, the air mass at the time of the observation, the total integration time and the Bright Star number of the star used for the determination of the instrumental response. Full details on the observing conditions and the data reduction procedure have been given in VDA and will not be repeated here.

For each star of table I there is a tracing of the observed spectrum where a quantity directly proportional to F_λ is plotted as a function of wavelength from λ 6150 Å to λ 10350 Å (Figs. 1a to 1d). The positions and the identifications of the strongest lines are given for the top spectrum of each page. The stars being ordered according to their spectral type, the identification on the unmarked spectra can be easily made using the top spectrum of the page. The line strengths of the most prominent lines are given in tables IIa and IIb. In these tables, column 1 gives an appreciation of the strength of the atmospheric absorption bands, column 2 the line identifications (for more details see VDA), columns 3 and the following the result of the measurements i.e. the observed wavelength, the equivalent width (W_λ) and a value proportional to the intensity of the line (I) i.e. proportional to $\int F_\lambda \, d\lambda$, the proportionality factor being constant for a given star but varying from one star to the other.

3. Discussion.

3.1 THE SPECTRA. — The spectrum of the galactic WN8 star WR40 is displayed here (Fig. 1a) because of its rather striking similarity to the one of the LMC WN8 star Br13, while both of them are markedly different from the spectrum of the galactic WN8 star WR55 (the spectrum of which is given in VDA).

In the latter star, the He II lines are much stronger than in WR40, while the He I lines are weaker. The same applies to the ratio between the NIV lines and the NIII lines which is higher in WR55 than in WR40. These two facts point to a higher temperature in the wind of WR55 than in the one of WR40 (and Br13). It may be worth noting that there is no detectable trace of H in WR55 while WR40 and Br13 have a remarkably high H/He ratio (Conti *et al.*, 1983 and present analysis, see below).

The heterogeneity of the spectroscopic properties in a given subtype is illustrated again in the next subtype with the spectrum of the galactic WN7 star WR78 which has stronger NIV lines and weaker He I lines than the WN7 star WR12 displayed in VDA. Again WR12 has a much stronger H signature than WR78.

By comparison to the WN8 spectra, the spectrum of the WN9-10 LMC star Br91 is nearly featureless. Neglecting the omnipresent H_α (+He II ?), the only strong emissions are due to He I. There is no clear He II signature and only a weak NIV signature, much weaker than the one observed in the 03If* star HD 93129 A (see VDA). Obviously the near infrared spectrum of Br91 can only confirm the uncertain nature of this kind of object, lying in the "no man's land" between the Of and WR stars.

The near infrared spectrum of HD 93129 A is amazingly similar to the one of the LMC WN4.5 + OB Br73 which has recently been shown to be an aggregate of several stars (Testor *et al.*, 1988). Basically both are characterized by three emissions, namely H_α + HeII λ 6560, NIV $\lambda\lambda$ 7103-7128 and HeII λ 10124, and by weak H absorption lines of the Paschen series. The NIV and He II signatures are much weaker than in the other WN4 - WN4.5 objects of our sample : WR7 (this paper), WR10 and WR31 (both in VDA). The comparison with WR31 is particularly instructive in the sense that it is a WN4 + O7 star where we have a weakening of the equivalent widths of the emissions due to the dilution effect by the O star continuum. Even so, these emissions remain quite strong relative to what we observe in Br73 which tends to indicate that most of the stars of the Br73 aggregate are not WR stars.

The SMC stars give access to earlier subtypes. Unfortunately all these SMC objects are classified as binaries and the WN signature is diluted by the O contribution. This is probably the reason of the striking weakness of the He II signature in SMC 6 and SMC 7. The same must also apply for the lack of NIV signature (observed in all the WN4s of our sample and in WR46, a WN3 pec) as the absence of NV signature (observed in WR46) does not allow to explain the lack of NIV signature by a shift in the ionization balance. As a matter of fact, the nearly featureless spectra of SMC 6 and SMC 7 are more reminiscent of the spectra of an O star than of that of a WN. This could indicate that we are dealing with unresolved aggregates of stars whose population is not dominated by WR-type objects.

The spectrum of SMC 5 is somewhat richer. The NIV signature is stronger than in the galactic WR46, with a corresponding weakening of the NIII signature. Two HeI lines show up as emissions, while in the visible spectrum the lines of that element are reported in absorption (Breysacher, 1988). The visible spectrum of that eclipsing binary is known to be variable (Breysacher, 1988) and we can expect the same in the near infrared. Therefore a systematic survey at different phases would be desirable before any detailed discussion of the spectrum can be made.

3.2 THE HYDROGEN SIGNATURE. — The lack of apparent signature of H in most of the WR stars as well as the enhanced strength of some CNO lines form the basis of the commonly accepted view that WR stars are highly evolved objects. In Conti's scenario (1976) WR stars are the result of the evolution of massive O stars which have undergone an appreciable mass loss by stellar wind ("onion skin" model). Within the frame of such a scenario "transition" objects have been defined, i.e. stars intermediate between plain O stars and fully developed WRs. Going backward from the latter, one spectral characteristic one would expect from the transition WR is a more or less weak H signature, just before the removal of the last layers containing this element. In some WN stars, such a signature is indeed observed. The most commonly quoted is the enhancement of the HeII emission lines of the Pickering series $(n-4)$ corresponding to even values of n relative to those lines corresponding to odd values of n. This enhancement is interpreted as the result of a blending of the even lines with the H I Balmer lines $(n-2)$. If this interpretation is generally accepted, the next step which consists in a quantitative determination of the H content of the wind (which is an indication of how far the star is in the transition) is more controversial. The reason is, as usual, that a quantitative analysis implies some assumptions as no direct knowledge exists concerning the tridimensional temperature and density (velocity) structure of the wind. Neglecting the possible influence of the underlying photospheric absorption spectrum, the simplest analyses refer to an isothermal and high temperature wind in which the lines under consideration are considered as optically thin or optically thick (Conti *et al.*, 1983, and references therein for previous works). A more recent study by Hillier (1987) of WR6 is based on a model in which the radiation transfer problem is treated in the case of a spherically expanding atmosphere.

This undoubtably represents an important step in the interpretation of the WR wind spectrum even if spherical symmetry and assumptions on the wind structure (velocity law) remain unavoidable. Such an analysis requires a considerable amount of computing time and consequently will only progressively become available for a large sample of stars. Fortunately the results published for WR6 indicate that a simple analysis lead to results which can be considered as reliable estimates of H^+/He^{++} : Hillier quotes an "excellent agreement" with the results obtained with the optically thick formula of Massey (1980) and an underestimation of the true H^+/He^{++} ratio with the assumption of optically thin emissions. For low abundances ($H/He < 0.2$) he quotes a "ratio accurate to 30 % without the need for detailed calculations". This is a level of accuracy quite acceptable if one keeps in mind that this is the order of magnitude of the error bars quoted by Conti *et al.* (1983). There is in fact little hope to see the accuracy of the observations improved since a fair part of the uncertainties is independent of the instrumentation : it is linked to the definition of the continuum and to blending problems.

In such a context we have decided that it could be interesting not only to publish our near infrared observations of the H signature in the near infrared spectrum of some WN stars but also to try a coarse analysis of them, in the same way Conti *et al.* (1983) did in the visible. This will allow to check the consistency of such a coarse analysis on lines with definitely different characteristics.

The main difference concerns the gf values and the principal quantum numbers of the upper levels. H_γ is the highest member of the Balmer series that Conti *et al.* (1983) are able to use for all their galactic objects and half of their Magellanic ones (including the ones for which we have near infrared data). This means that, for the H lines, the log gf values lies between $+0.7098$ (H_α) and -0.4469 (H_γ) and that the maximum values of the principal quantum number of the upper levels is 5. In the near infrared we will mainly rely on lines with log gf between -1.0461 (P 11) and -1.2916 (P 13) and with principal quantum numbers of the upper levels higher than 10. This implies that better conditions are met : one may expect that the lines are optically thin and that (which is important) the population of the upper levels approaches that of an LTE distribution (departure coefficient close to 1). Concerning this last remark, it may be important to remember that the "optically thick formula" of Massey (1980) used by Conti *et al.* (1983) assumes, as the optically thin one, that all the departure coefficients are equal to 1. One could expect that this is hardly the case for many objects when dealing with lines such as H_α and H_β or their corresponding lines of the HeII series.

Another interesting characteristic of the near infrared lines we will use is that their wavelengths are rather close in the sense that they span a wavelength domain on which the variation of the differential reddening may be neglected ($A_\lambda/E(B-V)$ varies by nearly a factor 2 in the wavelength domain considered by Conti *et al.* (1983) while it varies by only a few percents in the near infrared domain we use).

For this study we have carefully examined our collection of near infrared spectra (i.e. not only the ones described here but also e.g. the ones of our first catalogue ; Vreux *et al.*, 1983) while searching for a clear indication of the presence of the H Paschen lines. We have indeed decided to limit ourselves to stars in which the H signature could be quantified i.e. we have discarded the objects for which the enhancement of the even lines relative to the odd ones was of the same order as the scatter of the data. This selection left us with eight stars, six Galactic ones and two Magellanic cloud ones.

An important step, before the measurements themselves, is the definition of the local continuum : as usual for WR stars, this is not always obvious. In this spectral region the difficulties linked to the intrinsic width of the emission lines (which can prevent to have access to the continuum due to the overlapping of the wings) are increased by the presence of many atmospheric absorption bands which forbid the use of large wavelength domains. Particularly annoying are the H_2O absorption bands disturbing the spectra from HeII 6-21 to nearly P 7 because, when getting again access to the continuum, it is in the 1 μm region i.e. a region where the effect of the infrared excess due to free emission can start to modify the slope of the continuum. Fortunately, in the situations where we had doubts about the position of the continuum, it happened that, if the choice could have a serious influence on the values of the equivalent width, its influence was much more limited on the ratio between the intensities of the odd and even members of the HeII $n-6$ series. For example, for the worst case, WR12, we have tried two extreme positions of the continuum leading to a variation of the order of 0.2 in the log EW but only of a variation of the order of 0.01 in the difference of the log between the odd and even series. In any case, when we had doubt about the position of the continuum, we made the measurements with what we considered to be the two extreme possible positions of the continuum and then we took the mean of the EWs obtained. It is that mean value which is given in table III and plotted in figure 2. The error bar, as explained above, is typically $< \pm 0.1$ in the log except for WR85 where it is close to twice that value.

The bulk of our analysis is based on the lines of the HeII $(n-6)$ series with n varying from 22 to 26, i.e., for H, on P 11, P 12 and P 13. Nevertheless, to increase our baseline, we have also measured the $15-6$ line which is only slightly weakened by the telluric bands. The influence of the latter has been estimated through the ratio of the continuum fluxes measured at the position of the $15-6$ line and shortward of P 7. The equivalent width of the blend P 7 + HeII $14-6$ was also measured. It is labelled as uncertain (brackets) when it is too severely perturbed by the wing of HeII λ 10124. On the short wavelength side, i.e. higher in the series than HeII $26-6$ (= P 13), the spectrum is again perturbed by different absorptions. There is already a rather clear one between P 13 and P 14. At shorter wavelengths they manifest themselves in some stars by the abrupt weakening of the lines corresponding to the transitions between $29-6$ and $34-6$ of HeII. Anyhow, that high in the series, serious blending problems exist between the different lines.

If the wind is optically thin at the wavelengths under consideration, a homogeneous line formation region produces fluxes which are given by

$$F_{\mathrm{ul}} \sim N_{\mathrm{u}}\, A_{\mathrm{ul}}\, h\nu_{\mathrm{ul}}$$

where N_{u} is the population of the upper level and A_{ul} the usual Einstein spontaneous emission coefficient. In the WR winds the electron densities are so high $\left(N_{\mathrm{e}} \sim 10^{12}\ \mathrm{cm}^{-3}\right)$ that it is generally accepted that collisional processes strongly dominate over the radiative ones to control the population of the higher levels of He^{+} (typically for $n > 10$, see for example Castor and Van Blerkom, 1970). In addition, the electron temperature is such that the exponential term in the Saha-Boltzmann equation is close to 1. As a consequence, $N_{\mathrm{u}}/g_{\mathrm{u}}$ can be considered as independent of u for the higher levels of He^{+} and the fluxes are merely proportional to

$$g_{\mathrm{u}}\, f_{\mathrm{ul}}\, \lambda_{\mathrm{ul}}^{-3}$$

where g_{u} is the statistical weight of the upper level and f_{ul} the oscillator strength of the transition under consideration.

Using this relation and the observed flux of HeII $15-6$, it is possible to predict the flux of any other line of the series. This has been done for the $24-6$ transition which, under the hypothesis explicited above, has a flux 4.71 times weaker than the $15-6$ transition. After division by the continuum, the resulting equivalent width has been plotted in figure 2 with a special symbol to indicate that it is not a directly observed EW. As can be seen, the predicted EW generally fit nicely with the EW of the $23-6$ and $25-6$ transitions. The use of the thick approximation (in the sense of Massey, 1980) leads to a result which differs by less than 20 % i.e. a variation which is not significant in the present context. A similar procedure has been applied to (HeII $14-6$ + P 7) which has been used to predict the EW of (HeII $20-6$ + P 10).

Two stars are worth a comment, namely WR16 and WR40. The graph related to the former in figure 2 indicates an intensity of HeII $25-6$ too high relative to the intensities of HeII $23-6$ and the predicted intensity of HeII $24-6$. This difference is important and, due to the high S/N ratio of the spectrum, we are confident that it is real even if we have not yet been able to identify the blending line which pushes up the apparent intensity of HeII $25-6$. We also think that the same applies to WR40 even if for this star we rely mainly on a predicted intensity of HeII $24-6$ as HeII $23-6$ is too severely blended by HeI $9d^3D-3p\ ^3P^0$ to allow a meaningful estimation of its intensity (for WR16 the HeI lines are weaker and the deblending consequently safer). These two stars share a common characteristic : in our sample they are the galactic WNs with the strongest HeI lines. Interestingly, Br13, which also has strong HeI lines, does not exhibit the same behaviour. It is tempting to link this to the fact that the NIII/NIV ratio (as indicated by the ratio of the lines of the two ions) is much stronger in the galactic stars then in Br13 and to suggest NIII as the blending component for the galactic stars.

For Br89, the difference between HeII $23-6$ and the value of He $24-6$ predicted from the observed intensity of HeII $15-6$ has to be considered as compatible with the error bar : for this star the spectrum is particularly noisy in the region of HeII $15-6$ and the error bar consequently much larger than usual.

For the stronger lines of the even members of the HeII $n-6$ series the situation is less critical. Let us simply remember that for stars with strong CIV lines, the P 11 + HeII $22-6$ blend can be slightly enhanced by a CIV line and that the P 13 + HeII 26 − 6 blend can be slightly weakened by the absorption between P 13 and P 14.

The next step is to derive from our data an estimation of the H^+/H_e^{++} number ratio to compare it with the previously published values of Conti *et al.* (1983). Under the hypothesis mentioned above, this can be done through a relation identical to the one used in the visible i.e.

$$\frac{F\,(\mathrm{H})}{F\,(\mathrm{He}^+)} = \frac{N\,(\mathrm{H}^+)}{N\,(\mathrm{He}^{++})}$$

as the $g_{\mathrm{ul}}\,A_{\mathrm{ul}}$ of the corresponding lines of the HeII $n-6$ and of the H $n-3$ series are nearly identical. In this relation $F\,(\mathrm{H})$ and $F\,(\mathrm{He}^+)$ respectively are the contributing fluxes of H and He^+ at the wavelength under consideration. Due to the very limited spectral range spanned by the lines used in this analysis, the continuum does not vary very much and the fluxes are roughly proportional to the EW given in table III, except for HeII 14 − 6 + P 7 and HeII 15 − 6 which are further away. For the unblended lines of HeII, as they are very few, we have used all the information available i.e. we have taken the mean of the observed intensities of HeII 23 − 6, 25 − 6 and 24 − 6 this last one being computed from the observed intensity of HeII 15 − 6 (see above). When all the lines were not available, we have used the thin model approximation to compute the intensity of the 24 − 6 transition from all the available data and then have taken the mean. For the blended lines of H+He^+ we have used the mean of the observed intensities of P 11 (+ HeII 22 − 6), P 12 (+ HeII 24 − 6) and P 13 (+ HeII 26 − 6). The resulting estimations of the H^+/He^{++} number ratio are given in table IV. The first column gives the identification of the star, the second the spectral type, the third the result of the present study. The number ratio derived by Conti *et al.* (1983) from their analysis of visible spectra are given in the next two columns respectively in the thin and thick approximations. For this comparison we have used the data plotted of the figures 8 to 11 of Conti *et al.* (1983) and not the numbers given in tables IV and V as, in some cases, these numbers take into account an (unquoted) estimation of the H^+/He^{++} ratio (Conti, private communication). The agreement between the Paschen and Balmer determinations is good in the sense that our value generally is in the range defined by the thin and thick approximations of Conti *et al.* (1983). We cannot expect a better agreement since the variety of slopes exhibited in the different graphs displayed in the figures 8 to 11 of Conti *et al.* (1989) clearly indicate that simple approximations are not sufficient to handle the Balmer series. As explained above we can expect to be in a better position with our data.

As a conclusion, the present discussion of the near infrared region not only confirms the results previously obtained but tends to indicate that in many cases the lower limit of the H^+/He^{++} ratio deduced from the analysis of the visible region has to be pushed higher up. We have not attempted to derive the H^+/He^{++} ratio using the Saha-Boltzmann equation and the intensities of some HeI and HeII lines as we consider that such an evaluation should better wait complete modelling of the wind of these stars.

Acknowledgements.

This research has been partly supported through a grant of the Fonds National de la Recherche Scientifique to J. M. Vreux and through NSF grant 88-06594. The tracings have been made at the Computing Center (SEGI) of Liège University. J. M. Vreux would also like to thank the Institut d'Astrophysique de Paris for its hospitality during the data processing. The stay of K. Rochowicz at the Institut d'Astrophysique in Liège has been supported by Liège University. The comments of J. Breysacher and J. P. Swings have also been appreciated.

References

ABBOTT D., CONTI P. : 1987, *Ann. Rev. Astron. Astrophys.* **25**, 113.
BREYSACHER J. : 1988, Ph. D. thesis, Université de Paris VII.
CASTOR J., VAN BLERKOM D. : 1970, *Astrophys. J.* **161**, 485.
CONTI P.S. : 1976, Mém. Soc. Roy. Sci. Liège, 6ème série, tome IX, 193.
CONTI P.S., LEEP E. M., PERRY D. N. : 1983, *Astrophys. J.* **268**, 228.
CONTI P.S., MASSEY P. : 1989, *Astrophys. J.* **337**, 251.
DENNEFELD M., GUTTIN LOMBARD B., LE LUYER M., ROSSIGNOL P. : 1979, ESO Technical Note IDG 120-79.
HILLIER D. J. : 1987, *Astrophys. J. Suppl. Ser.* **63**, 965.
MASSEY P. : 1980, *Astrophys. J.* **236**, 256.
SCHMUTZ W., HAMANN W.-R., WESSOLOWSKI V. : 1989, *Astron. Astrophys.*, **210**, 236.
TESTOR G., LLEBARIA A., DEBRAY B. : 1988, *The Messenger* **54**, 43.
VAN DER HUCHT K. A., CONTI P. S., LUNDSTRÖM I., STENHOLM B. : 1981, *Space Sci. Rev.* **28**, 227.
VAN DER HUCHT K. A., WILLIAMS P. M., THÉ P. S. : 1987, *Q J R Astron. Soc.* **28**, 254.
VREUX J. M., DENNEFELD M., ANDRILLAT Y. : 1983, *Astron. Astrophys. Suppl. Ser.* **54**, 437.
WESSOLOWSKI V., SCHMUTZ W., HAMANN W.-R. : 1988, *Astron. Astrophys.*, **194**, 160.

TABLE I. — *Journal of observations.*

The L.M.C. stars

Spectral Type	Br number	HD number	V	Date	Air mass	Integration time (sec)	Standard for reduction
WN8	13	33133	12.6	17.11.81	1.34	3000	HR 718
WN7	26	36063	12.9	17.11.81	1.62	2400	HR 718
WN4.5+OB	73		12.2	28.11.80	1.44	3600	HR 8518
WN7	89	38282	11.1	27.11.80	1.30	2400	HR 8518
WN9-10	91		12.0	17.11.81	1.42	1800	HR 718

The S.M.C. stars

Spectral Type	SMC/AB	HD number	V	Date	Air mass	Integration time (sec)	Standard for reduction
WN4+O7I	5	5980	11.9	27.11.80	1.36	3600	HR 8519
WN3+O7Ia	6		12.4	27.11.80	1.47	3600	HR 8519
WN4+OB	7		13.2	28.11.80	1.36	5400	HR 8518
WC4?+O4	8		13.0	17.11.81	1.40	1800	HR 718

The Galactic stars

Spectral Type	WR number	HD number	V	Date	Air mass	Integration time (sec)	Standard for reduction
WN4	WR 7	56925	11.7	22.5.80	1.78	120	HR 4963
WN8	WR 40	96548	7.8	20.5.80	1.23	120	HR 4963
WN7	WR 78	151932	6.6	21.5.80	1.13	60	HR 4963

TABLE IIa. — *Wavelength, equivalent width and intensity of the strongest emission lines in a sample of late WN stars.*

Atmos. abs.	Identification	Br 89 - WN6 A.M. : 1.30			WR 78 - WN7 A.M. : 1.13			Br 26 - WN7 A.M. : 1.62			WR 40 - WN8 A.M. : 1.23			Br 13 - WN8 A.M. : 1.34			Br 91 - WN9 A.M. : 1.42		
		λ	W	I	λ	W	I	λ	W	I	λ	W	I	λ	W	I	λ	W	I
	N IV 6212-6219	6223	0.6	0.6	6215	1.7	2.8	6236	1.5	1.8	6216	0.7	1.6	6220	0.8	1.5			
	He II 6234	6241	0.3	0.3	6233	0.8	1.3				6237	1.0	2.4	6241	0.8	1.5			
	He II 6406	6415	0.6	0.6	6406	0.8	1.3	6415	2.5	2.5	6407	1.2	2.8	6413	1.0	2.0			
W.	N III 6450-6460				6460	0.8	1.3				6475	7.0	16.	6461	0.8	1.6	6466	1.3	1.3
	He II 6560 H_α 6563	6568	74.0	72.0	6562	37.0	57.5	6570	68.0	68.0	6564	95.0	212.	6569	100.0	170.0	6570	57	58
	He I 6678 He II 6683	6685	6.5	6.0	6679	10.0	16.0	6689	11.0	11.0	6680	53.0	113.	6684	24.0	38	6685	14	14
W.W.	C IV 7062 He I 7065	7070	5.5	4.0	7065	6.4	9.2	7077	9.0	7.5	7068	38.0	76.	7073	16.0	22.0	7074	85	85
	N IV 7103-7128	7122	18.5	13.0	7113	17.0	24.0	7123	36.0	30.0	7115	14.0	28	7120	18.0	24.0			
Str.	He II 7177	7185	4.0	3.0	7177	1.7	2.4	7185	6	5				7185	5.0	7.0			
W.	N III 8019										8018	1.0	1.8						
Str.	He II 8237	8249	8.5	3.5	8240	5.7	6.1	8250	15.0	7.5	8243	5.1	8.8	8247	8.0	7.0			
	C IV 8859 He II 8859 P_{11} 8863	8871	1.2	0.4	8860	1.0	1.0	8866	2.4	1.0	8857	3.5	4.8	8869	3.0	2.0			
	He II 10045 P_7 10049	10059	10.0	2.5	10050	9.0	6.5	10062	12.0	4.0	10045	31.0	33.5	10058	19.0	10.0			
	He II 10124	10133	87	21.5	10125	57.0	42.0	10137	107.0	34.0	10128	33.0	36.1	10134	38.0	20.0			

Note to table IIa : The wavelengths (λ) and equivalent widths (W) are given in Angström units. The intensity (I) is in arbitrary units.

TABLE IIb. — *Wavelength, equivalent width and intensity of the strongest emission lines in a sample of early WN stars and an* 03If*.

Atmos abs.	Identification	WR 7 - WN4 A.M. : 1.78			Br 73 - WN4.5+OB A.M. : 1.44			SMC 5 - WN3pec+OB A.M. : 1.36			SMC 6 - WN3+O7Ia A.M. : 1.47			SMC 7 - WN3+OB A.M. : 1.36			HD 93129A - O3If* A.M. : 1.61		
		λ	W	I	λ	W	I	λ	W	I	λ	W	I	λ	W	I	λ	W	I
	N IV 6212-6219																6214	.5	7.
	He II 6234	6227	4.5	3.0															
	He II 6406	6404	7.0	4.5															
W	N V 6479	-	-	-															
	He II 6560 H_α 6563	6561	137.0	88.0	6570	10.5	16.5	6566	43.0	145.	6565	7.0	16.5	6563	8.5	7.0	6567	7.5	115.
	He I 6678 He II 6683	6684	13.0	8.5				6677	3.5	11.									
Str.	He II 6891	6898	11.5	7.0															
	N IV 7103-7128	7114	88.	52.	7121	4.0	6.0	7117	14.0	37.							7112	3.5	50
Str.	He II 7177	7176	24.	14.															
Str.	N IV 7583 He II 7593	7578	12.0	6.5															
Str.	N IV 7705 O VI 7717 C IV 7726	7710	3.5	2.0															
Str.	He II 8237	8238	52.0	25.0				8246	12.0	15.									
	He II 10124	10128	414.0	145.0	10140	10.0	7.5	10129	113.5	86.	10133	16.5	8.0	10127	26.0	7.0	10121	1.5	12.

Note to table IIb : The wavelengths (λ) and equivalent widths (W) are given in Angström units. The intensity (I) is in arbitrary units.

TABLE III. — Log EW (mA).

	6-14 P7	6-15	6-22 P11	6-23	6-24 P12	6-25	6-26 P13
WR 12	4.43	3.41	3.79	2.91	3.62	2.77	3.33
WR 16	4.26	3.09	3.58	2.48	3.46	2.72	3.16
WR 22	3.78	2.63	2.87	2.0	-	-	-
WR 40	4.44	3.13	3.69	-	3.60	2.65	3.46
WR 78	(3.74)	3.17	3.12	2.53	2.86	2.52	2.53
WR 85	4.24	3.49	3.59	2.92	3.30	2.76	2.79
Br 13	4.36	3.48	3.68	2.85	3.52	2.59	3.34
Br 89	(3.97)	3.30	3.28	2.38	3.11	-	3.00

TABLE IV. — H^+/He^{++}.

Object	Spectral type	This paper	Conti et al. (1983)	
		Thin model	Thin model	Thick model
WR 12	WN 7	5	-	-
WR 16	WN 8	6.5	3.7	9.2
WR 22	WN7+abs	5	3.8	9.5
WR 40	WN 8	9	3.6	8.9
WR 78	WN 7	1.5	1.2	2.3
WR 85	WN 8	2	0.9	1.6
Br 13	WN 6	5	4.5	11.9
Br 89	WN 9	3.5	2.5	5.5

Remark : The decimals are given to keep a numerical consistency between the thin and thick evaluations. They are not representative of the accuracy of the determination (see Conti *et al.*, 1983).

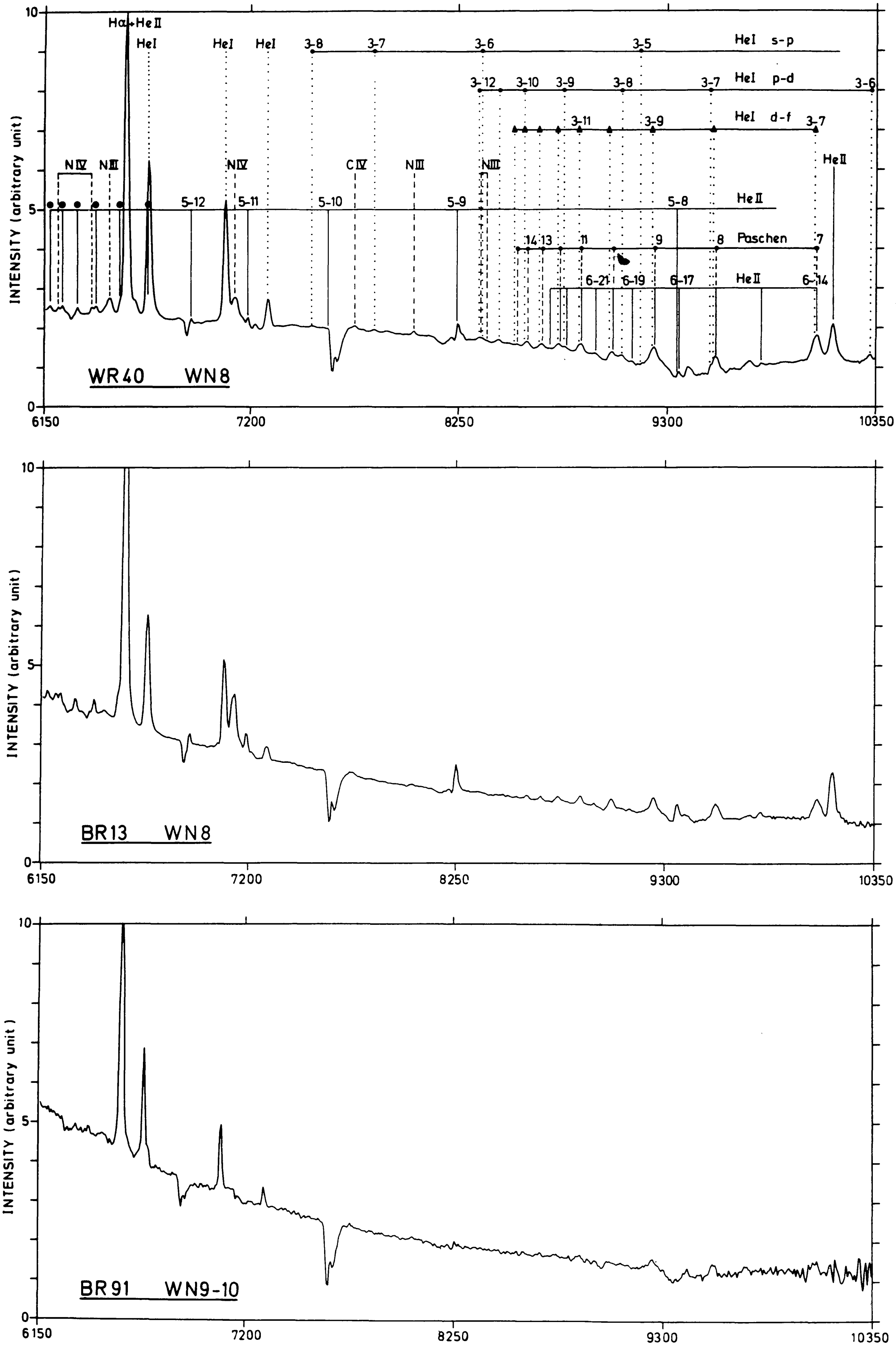

FIGURE 1. — Spectra of a sample of galactic and Magellanic WR stars.

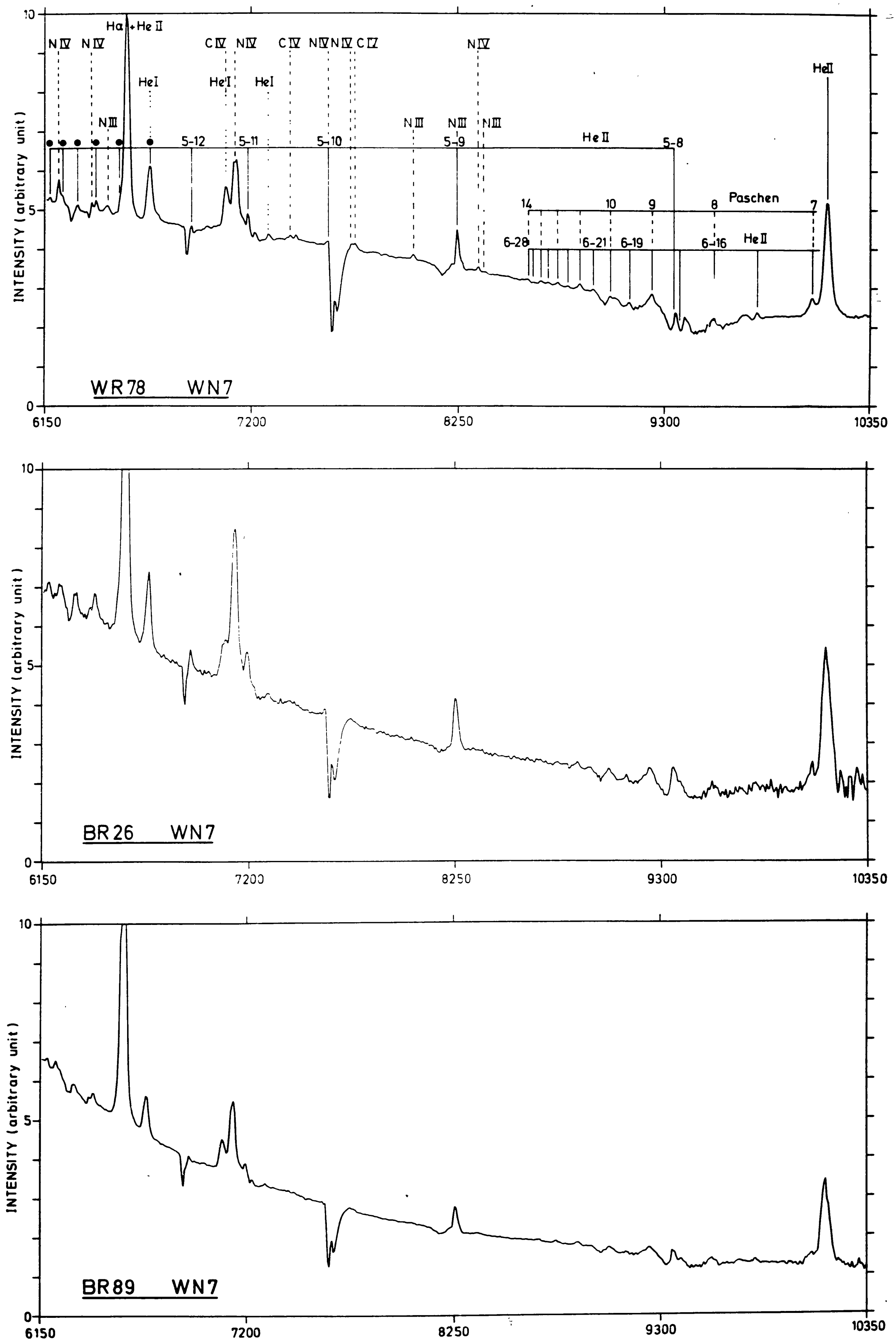
INTENSITY (arbitrary unit)
WR78 WN7
BR26 WN7
BR89 WN7
Hα + He II
N IV
N III
He I
C IV
5-12
5-11
5-10
5-9
5-8
He II
Paschen
14
10
9
8
7
6-28
6-21
6-19
6-16
6150
7200
8250
9300
10350

FIGURE 1b.

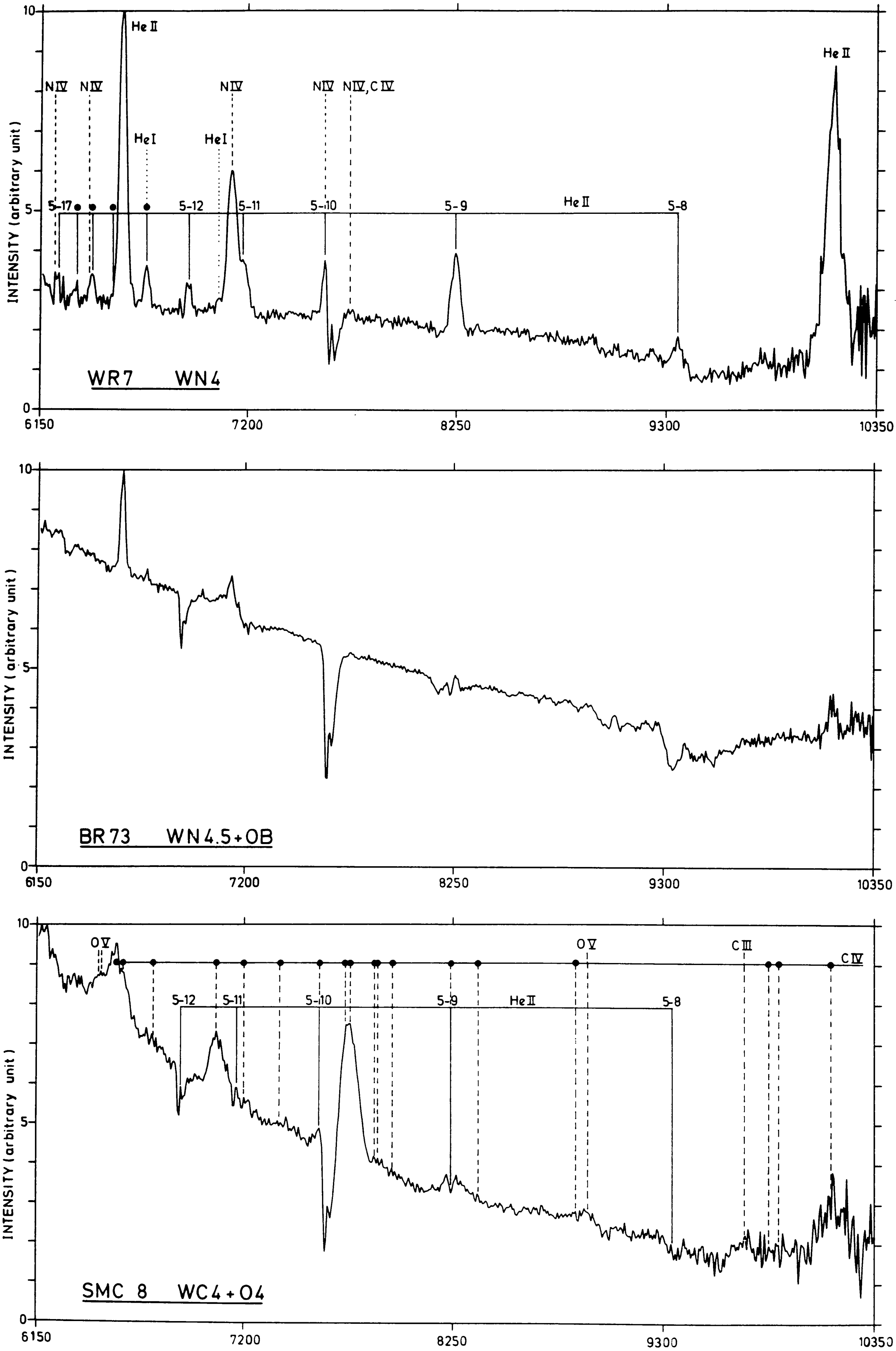
INTENSITY (arbitrary unit)
He II
N IV
N IV
He I
He I
N IV
N IV
N IV, C IV
5-17
5-12
5-11
5-10
5-9
He II
5-8
He II
WR7 WN4
6150
7200
8250
9300
10350
BR73 WN4.5+OB
O V
O V
C III
C IV
SMC 8 WC4+O4

FIGURE 1c.

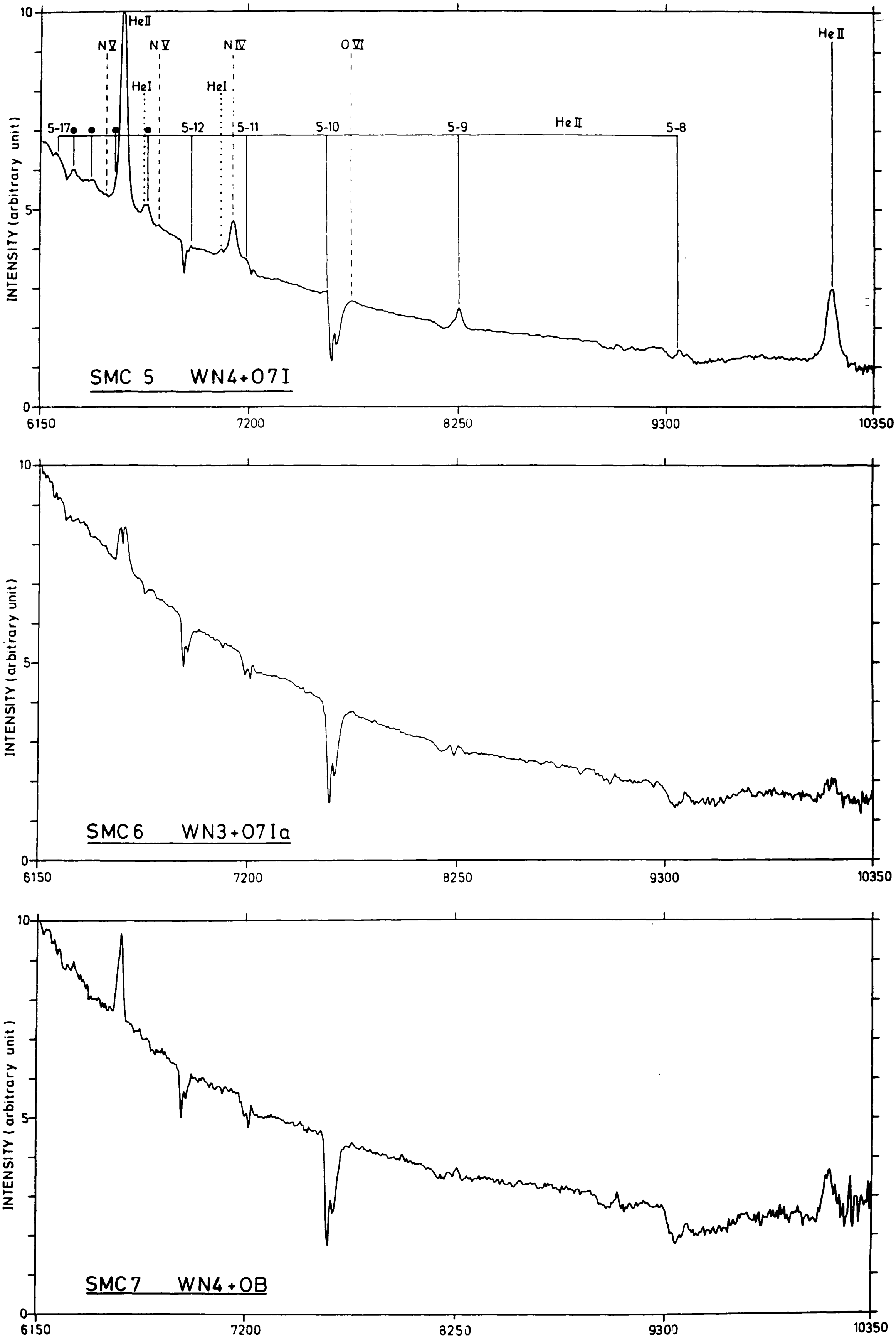

HeII
NV
NV
NIV
OVI
HeI
HeI
HeII
5-17
5-12
5-11
5-10
5-9
HeII
5-8
INTENSITY (arbitrary unit)
SMC 5 WN4+O7I
SMC 6 WN3+O7Ia
SMC 7 WN4+OB
0
5
10
6150
7200
8250
9300
10350

FIGURE 1d.

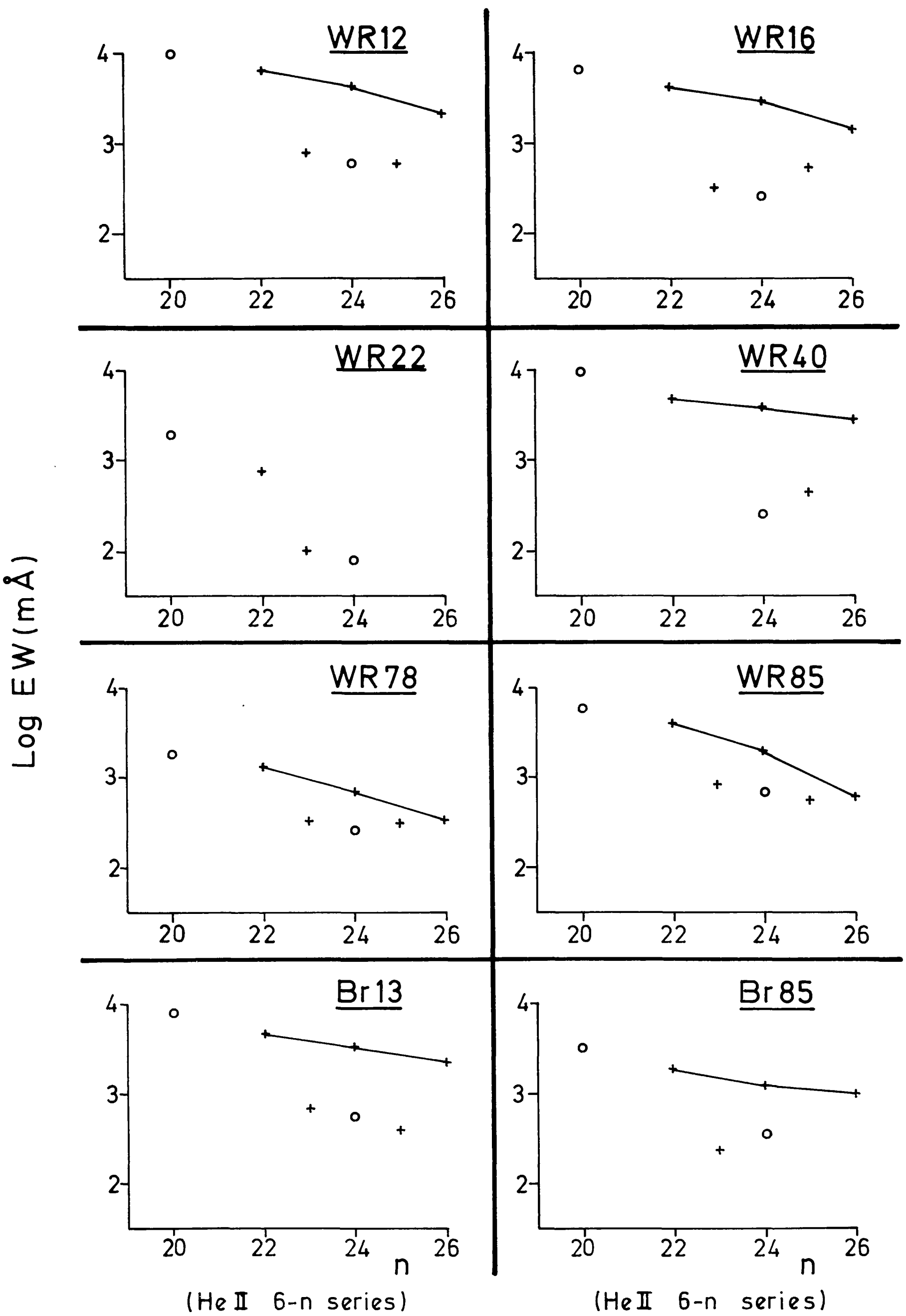

FIGURE 2. — Logarithm of the equivalent width (EW) as a function of principal quantum number of HeII $n-6$ series. *Crosses :* measured EW_S. The crosses corresponding to HeII lines with an even quantum number have been linked by straight lines to make their identification easier and better illustrate their reinforcement by the corresponding H Paschen lines. *Circles* have been used for the EW of HeII 24 – 6 and HeII 20 – 6 (+ P 10) which have been calculated respectively from the intensities of HeII 15 – 6 and HeII 14 – 6 (+ P 7) in the hypothesis of optically thin lines and LTE (see text).